© 2019. Published by The Company of Biologists Ltd | Journal of Cell Science (2019) 132, jcs229054. doi:10.1242/jcs.229054

RESEARCH ARTICLE

Tau interacts with SHP2 in neuronal systems and in Alzheimer's disease brains

Yohan Kim[1,*], Guanghao Liu[2], Chad J. Leugers[1,‡], Joseph D. Mueller[1], Meghan B. Francis[1], Marco M. Hefti[3], Julie A. Schneider[4] and Gloria Lee[1,2,§]

ABSTRACT

Microtubule-associated protein tau, an integral component of neurofibrillary tangles, interacts with a variety of signaling molecules. Previously, our laboratory reported that nerve growth factor (NGF)-induced MAPK activation in a PC12-derived cell line was potentiated by tau, with phosphorylation at T231 being required. Therefore, we sought to identify a signaling molecule involved in the NGF-induced Ras-MAPK pathway that interacted with phospho-T231-tau. Here, we report that the protein tyrosine phosphatase SHP2 (also known as PTPN11) interacted with tau, with phospho-T231 significantly enhancing the interaction. By using proximity ligation assays, we found that endogenous tau–SHP2 complexes were present in neuronal cells, where the number of tau–SHP2 complexes significantly increased when the cells were treated with NGF, with phosphorylation at T231 being required for the increase. The interaction did not require microtubule association, and an association between tau and activated SHP2 was also found. Tau–SHP2 complexes were also found in both primary mouse hippocampal cultures and adult mouse brain. Finally, SHP2 levels were upregulated in samples from patients with mild and severe Alzheimer's disease (AD), and the level of tau–SHP2 complexes were increased in AD patient samples. These findings strongly suggest a role for the tau–SHP2 interaction in NGF-stimulated neuronal development and in AD.

This article has an associated First Person interview with the first author of the paper.

KEY WORDS: Tau, SHP2, NGF, Tau phosphorylation, Alzheimer's disease

INTRODUCTION

Microtubule-associated protein tau was initially described as a protein that promoted the polymerization and stabilization of microtubules (Weingarten et al., 1975; Witman et al., 1976) with phosphorylation negatively regulating its ability to interact with microtubules (Lindwall and Cole, 1984). Subsequently, more functions for tau have emerged, with tau phosphorylation again having a regulatory role. We have reported that tau associated with Src family non-receptor tyrosine kinases (SFKs) and was tyrosine phosphorylated by Fyn on Y18 (Lee et al., 1998, 2004). Tyrosine phosphorylation of proteins is intimately involved in regulating signal transduction and our finding suggested that tau might be involved in signal transduction (reviewed in Lee, 2005). If so, it would be important for the tyrosine phosphorylation of tau to be regulated, suggesting that tau might be a substrate for a protein tyrosine phosphatase.

Interest in the tyrosine phosphorylation of tau has also stemmed from our finding that phosphorylated (p)Y18-tau was found in the neurofibrillary tangles of Alzheimer's disease (AD) patients, in parallel with the well-described appearance of tau phosphorylated on serine and threonine residues. Neurofibrillary tangles were positive for pY18-tau. However, double-labeling samples with antibody AT8, which labels pS199/S202/T205 residues, suggested that some pathological tau, such as that present in neuropil threads, does not contain pY18 (Lee et al., 2004). Among the possible explanations for the absence of pY18-tau would be the participation of a protein tyrosine phosphatase. Among these proteins is SHP2 (also known as PTPN11), a protein tyrosine phosphatase that is essential for full activation of the MAPK pathway, a critical part of downstream signaling from many receptor tyrosine kinase pathways (reviewed in Tajan et al., 2015). While SHP2 is ubiquitously expressed, it has been reported to play a critical role for synaptic plasticity and memory formation (Kusakari et al., 2015), in addition to growth factor-mediated signal transduction associated with neuronal differentiation. Moreover, the role of SHP2 in the nerve growth factor (NGF)-induced MAPK pathway in PC12 cells parallels that of tau. In PC12 cells, just as tau is required for NGF-dependent neurite outgrowth (Esmaeli-Azad et al., 1994) and MAPK activation (Leugers and Lee, 2010), SHP2 has also been found to be required for both properties in PC12 cells (Wright et al., 1997). Similar to what is seen for tau, where introducing active Ras rescues MAPK activation in a tau-depleted cell line (Leugers and Lee, 2010), the absence of functional SHP2 impaired growth factor-induced Ras activation, suggesting that SHP2 also acts upstream of Ras (Shi et al., 2000). Given such similarities in the signaling roles of tau and SHP2 in differentiating neuronal cells, we have investigated their relationship. Here, we report the interaction between tau and SHP2, and investigate the nature of the interaction and the effect of tau phosphorylation at T231. We examine the interaction in PC12-related PC6-3 cells, primary mouse hippocampal neurons and in mouse brain. After detecting the presence of the tau–SHP2 interaction in developing neurons, we evaluated human brain sections from patients with mild or severe AD, and found that in these AD samples, SHP2 was upregulated and often colocalized with neurofibrillary tangles. We also found evidence supporting an increase in the tau–SHP2 interaction during AD. Our data allows us to speculate that the tau–SHP2 interaction has a role in neurodegeneration.

[1]Department of Internal Medicine, University of Iowa Carver College of Medicine, Iowa City, IA 52242, USA. [2]Interdisciplinary Program in Neuroscience, University of Iowa Carver College of Medicine, Iowa City, IA 52242, USA. [3]Department of Pathology, University of Iowa Carver College of Medicine, Iowa City, IA 52242, USA. [4]Department of Pathology, Rush Medical College, Chicago, IL 60612, USA. *Present address: Nathan S. Kline Institute for Psychiatric Research, Orangeburg, NY 10962. ‡Present address: Department of Biology, Morningside College, Sioux City, IA 51106.

§Author for correspondence (gloria-lee@uiowa.edu)

G.Lee, 0000-0002-8633-1534

Received 20 December 2018; Accepted 5 June 2019

Journal of Cell Science (2019) 132, jcs229054. doi:10.1242/jcs.229054

RESULTS

Tau association with SHP2 in neuronal and non-neuronal cells

To determine whether tau associated with SHP2, we performed co-immunoprecipitations (co-IPs) using D5 cells [PC6-3 cells stably expressing the 3-repeat (3R) tau isoform] and a phospho-specific tau antibody (Fig. 1A). We found SHP2 in the immunoprecipitated proteins, suggesting a tau–SHP2 interaction. To confirm the interaction, we also performed a co-IP using COS7 cells where 3R tau, expressed by transient transfection, was immunoprecipitated by DA9, an antibody recognizing total tau (Fig. 1B); control immunoprecipitations were performed with mock-transfected cells. Endogenous SHP2 co-immunoprecipitated with the expressed tau, confirming the tau–SHP2 association. To provide additional evidence for the tau–SHP2 interaction, we also performed an *in vitro* binding assay where the requirement for phosphorylated tau could be tested. Purified *E. coli*-synthesized non-phosphorylated 3R tau was added to SHP2 immunoprecipitated from COS7 cells. As controls, *E. coli*-synthesized tau was also added to immunoprecipitations performed with anti-paxillin or control IgG antibody. After washing the binding reactions, proteins bound to the immunoprecipitated SHP2 or paxillin were examined. The *in vitro* binding assay showed that there was an association between *E. coli*-synthesized non-phosphorylated tau and SHP2 (Fig. 1C). To determine whether phosphorylation affected the association, we compared the binding of *E. coli*-synthesized phosphomimetic tau (T231D) to that of wild-type (WT) tau; T231D tau was chosen since our initial co-IP used an antibody against pT231 tau (CP17, Fig. 1A). When equal amounts of T231D tau or WT tau were incubated with SHP2 immunoprecipitated from COS7 cells, after identical washing steps, we found that T231D tau bound to SHP2 more avidly (Fig. 1D). In fact, T231D tau bound to SHP2 at a level that was ∼12-fold higher than WT tau as determined by densitometry ($P<0.001$). Taken together, these results demonstrate that although phosphorylation of tau is not required for the tau–SHP2 association, it is likely that phosphorylation at T231 significantly enhances SHP2 association.

Tau as a substrate for SHP2

The ability of SHP2 to dephosphorylate tau was examined using *E. coli*-synthesized full-length 3R tau that had been phosphorylated *in vitro* on Y18 using Fyn kinase (Lee et al., 2004). Following the addition of PP2 to inhibit additional Fyn activity, the phosphorylated tau protein was incubated with purified SHP2 (obtained commercially). The reaction was then examined by immunoblot analysis using 9G3, a monoclonal against pY18 tau. We found that the level of pY18 tau was reduced upon incubation with SHP2 (Fig. 2), indicating that pY18 tau is dephosphorylated by SHP2. As confirmation, we examined the ability of SHP2 to dephosphorylate a pY18-tau peptide. Controls included the tau peptide not phosphorylated at pY18 and boiled SHP2, where SHP2 catalytic activity was dead. We found that incubation with active SHP2 reduced levels of pY18 tau peptide whereas incubation with boiled SHP2 did not (Table S2). Together, our findings indicate that pY18 tau is a substrate for SHP2.

Localization of tau–SHP2 complexes in cells

To investigate tau–SHP2 complexes at the single-cell level, we utilized *in situ* proximity ligation assays (PLAs). PLAs provide a sensitive and specific probe for protein–protein interactions *in situ* since PLA signals are recovered only when the two PLA probes lie within 40 nm of each other (Söderberg et al., 2006, 2008). PLAs were conducted on fixed PC6-3 cells using anti-tau (DA9) and anti-SHP2 antibodies, resulting in tau–SHP2 complexes being highlighted with

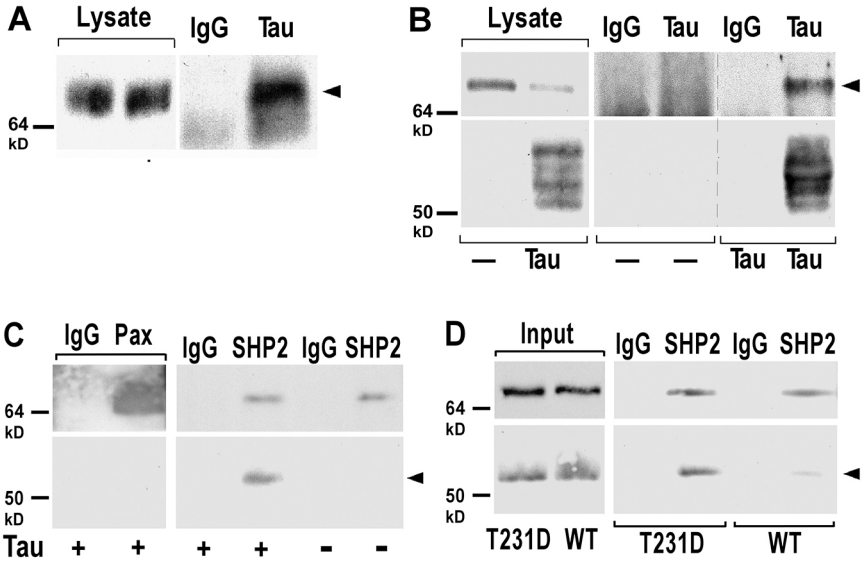

Fig. 1. Tau associates with endogenous SHP2, with the T231D phosphomimetic mutation enhancing SHP2 binding. (A) Lysates from D5 cells were subjected to immunoprecipitation with CP17, a monoclonal antibody specific for pT231 tau. The input lysates containing 1% of the total lysate (left panel) and immunoprecipitations (right panel) were both probed with anti-SHP2 antibody. (B) COS7 cells, expressing human WT tau (3R) or mock transfected (–), were immunoprecipitated with DA9, a monoclonal antibody against total tau. The immunoprecipitation (right panels) and input lysates (left panels) were probed with anti-SHP2 (upper panels) or with the total HRP–Tau5 antibody (lower panels). Input lysates (left panels) contained 0.1% of the total lysates. Arrowheads in A and B indicate SHP2. Control immunoprecipitation in A and B were performed with non-specific mouse IgG. (C) SHP2 or paxillin was immunoprecipitated from COS7 cells, using non-specific IgG as controls. *E. coli* synthesized WT tau was added (+) or not (–) and proteins bound to immunoprecipitated proteins were probed with the anti-human tau antibody tau13 (lower panels). As controls, the immunoprecipitated paxillin and SHP2 were probed with anti-paxillin (upper left panel) or anti-SHP2 (upper right panel). (D) As in C, SHP2 was immunoprecipitated from COS7 cells and *E. coli* synthesized WT tau or T231D tau mutant was added. Proteins bound to SHP2 were probed with Tau13 (lower right panel). As controls, 0.1% of the COS7 cell lysate and the immunoprecipitated SHP2 were probed with anti-SHP2 (upper left and right panels). Input tau proteins (lower left panel) were 0.5 µg of *E. coli* synthesized WT or T231D tau. Arrowheads in panels C and D indicate *E. coli* synthesized tau. In D, the exposure shown in the lower right panel, probed with Tau13, was a shorter exposure relative to that shown in panel C, lower right panel.

Journal of Cell Science (2019) 132, jcs229054. doi:10.1242/jcs.229054

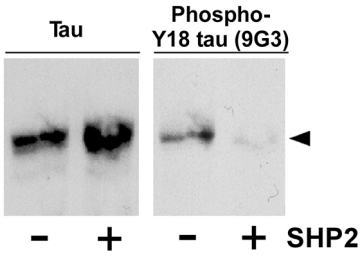

Fig. 2. Tau serves as a substrate for SHP2 *in vitro*. *E. coli* synthesized full-length tau was phosphorylated though incubation with Fyn (Millipore) and subsequently incubated with SHP2 as described in the Materials and Methods; the control reaction omitted SHP2. Tau was probed with 9G3 (right panel) and re-probed with total tau antibody (left panel). Arrowhead indicates tau.

a fluorescent orange indicator. Total tau was additionally detected by using Alexa Fluor 488-conjugated anti-mouse secondary antibody to label DA9. The data, as shown in confocal projections, illustrated a clear punctate pattern indicating endogenous tau–SHP2 complexes in non-stimulated PC6-3 cells (Fig. 3A); tau–SHP2 complexes were also visible in NGF-stimulated PC6-3 cells (Fig. 3B). By examining individual confocal layers, we could see that the PLA signals largely resided either underneath or to the side of the nucleus, with some at the edge of the cell (Fig. S1). By counting the numbers of puncta in both non-stimulated and NGF-stimulated cells, we found that relative to non-stimulated cells, NGF-stimulated PC6-3 cells exhibited a 69% increase in the number of tau–SHP2 complexes (Fig. 3E, left; P=0.0431); non-stimulated cells averaged 11.9 per cell while NGF-stimulated cells averaged 20.1 per cell. The association between endogenous tau and activated SHP2 was also examined using DA9 and anti-activated SHP2 antibody (Fig. 3C,D). In non-stimulated cells, only 7% of the cells had PLA puncta, averaging 1.04 per cell; this was not surprising since non-stimulated cells had very low levels of activated SHP2. In contrast, 33.8% of NGF-stimulated cells had PLA puncta, averaging 1.4 per cell, owing to the increased levels of activated SHP2 in stimulated cells (Fig. 3E, right). Finally, we examined complexes between pT231 tau and SHP2, using the antibody CP17 to detect pT231 (Fig. 3F), and found that the extent of the NGF-induced increase (67%; P=0.0208) was similar to that shown by the total tau-SHP2 PLA levels. Taken together, our data show that, in neuronal cells, NGF stimulation increased the level of association between endogenous tau and SHP2. Our data also demonstrated the association between tau and activated SHP2.

Tau–SHP2 complexes were further examined in COS7 cells where tau was transiently expressed. While COS7 cells expressing tau exhibited a high level of tau–SHP2 complexes (Fig. 4A), non-transfected cells exhibited very few puncta, confirming that tau was required for the PLA signal. To examine the association between tau and activated SHP2 in COS7 cells, PLA was conducted following EGF stimulation. As expected, the level of tau-activated SHP2 complexes was dramatically increased after EGF treatment (Fig. 4B, C). Interestingly, the complexes were mainly localized along the edge of the cells (Fig. 4C). To further examine this localization, actin filaments were labeled with phalloidin–Alexa-Fluor-488 (Fig. 4D). Many complexes colocalized with actin ruffles on the plasma membrane, suggesting a membrane localization for tau–SHP2 complexes in stimulated cells.

pT231 tau and SHP2 form complexes in NGF-stimulated cells and in primary hippocampal neurons

Previously, we have reported that NGF treatment increases the level of pT231 tau in D5 cells (Leugers and Lee, 2010). We confirmed this result for PC6-3 cells by using flow cytometry where CP17 was reacted to fixed and permeabilized cells. We found that following NGF stimulation, the level of pT231 tau was significantly increased (by 63%; P=0.0211). If phosphorylation at T231 leads to an increase in SHP2 association, such changes in pT231 tau levels would, in part, explain the observed increase in the levels of endogenous tau–SHP2 complexes after NGF stimulation (Fig. 3).

To examine the role of pT231 in SHP2 binding during NGF signaling, phosphomimetic tau (T231D), T231A mutant tau or WT tau was expressed in rTau4 cells (tau-depleted PC6-3 cells; Leugers and Lee, 2010). PLAs were then conducted on cells with or without NGF treatment. We found that regardless of the type of expressed tau, transfected rTau4 cells showed clear puncta representing tau–SHP2 complexes (Fig. 5A–D); non-transfected cells showed no puncta. For each transfection, we quantified the level of PLA signals in each cell, normalizing the PLA level to the level of tau expressed in that cell (70–90 cells were evaluated per transfection). After the average normalized level of PLA signals per cell was obtained for each culture, for each construct we calculated the NGF-induced fold increase in the level of PLA signals by calculating the ratio of PLA signal with NGF to that without NGF. We found that for T231D tau, the increase was 2.15-fold while for T231A, the increase was 1.18-fold, with a significant difference between T231D and T231A (Fig. 5E, P=0.0332). In addition, the increase in the level of PLA signals for WT tau–SHP2 complexes was always at an intermediate level (1.62, Fig. 5E), which very likely, resulted from an intermediate level of phosphorylation occurring at T231 for WT tau. Moreover, our data strongly suggested that phosphorylation at T231 was required for the increased amount of SHP2 association following NGF treatment.

Finally, we examined the role of microtubule binding for tau association with SHP2. The S262D/S356D double-mutant of tau, which lacks microtubule binding ability (Biernat et al., 1993; Drewes et al., 1995), was expressed in rTau4 cells and PLA was conducted, with quantification being performed as for the T231A and T231D mutants (Fig. 5F,G). Relative to WT tau, we found a statistically significant increase of 1.8-fold in PLA signals for the mutant ($P \leq 0.0001$), indicating that microtubule binding inhibited the ability of tau to associate with SHP2.

To examine the interaction between tau and SHP2 in primary cultured hippocampal mouse neurons, PLA was performed on neurons from WT mice, using neurons from tau-knockout (KO) mice as a control. To visualize neuronal processes, actin was labeled with phalloidin–Alexa Fluor 488. Tau–SHP2 complexes were found in both cell soma and neuronal processes of WT hippocampal neurons (Fig. 6A), and, as expected, little labeling was observed in the tau KO mouse (Fig. 6B). Interestingly, higher magnification of the primary neurons showed that tau–SHP2 complexes appeared to lie just adjacent to the processes (Fig. 6C, arrowheads). The precise localization of these complexes remains to be determined.

To investigate the association of pT231 tau with SHP2 in primary neurons, primary hippocampal neurons were subjected to PLAs using CP17 and anti-SHP2 antibodies, with PLA using DA9 and anti-SHP2 performed as a control. Complexes of pT231 tau and SHP2, and of total tau and SHP2 were present in both soma and processes (Fig. 6D, E). To characterize the localization in neurons, 50 cells of each culture were randomly chosen and the proportion of PLA puncta in processes or soma were calculated for each cell. While the pT231 tau–SHP2 complexes favored locating in the soma relative to neuronal processes, the total tau–SHP2 complexes were equally prominent in both soma and processes (Fig. 6F). In comparing the ratio of PLA puncta in processes to that in soma, for complexes of pT231 tau and

Journal of Cell Science (2019) 132, jcs229054. doi:10.1242/jcs.229054

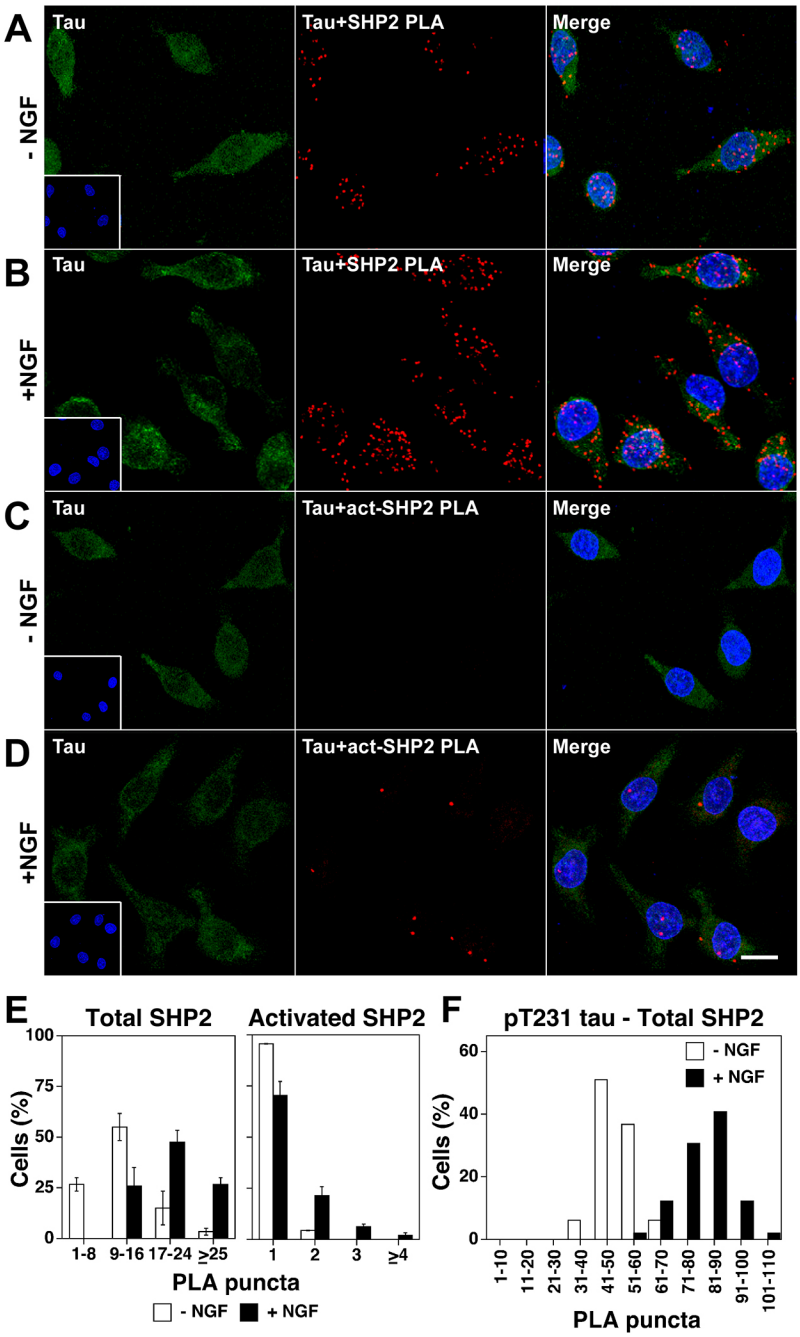

Fig. 3. Endogenous tau–SHP2 complexes are present as a punctate pattern in neuronal cells. (A–D) PC6-3 cells were stimulated with or without NGF for 5 min and subjected to PLA as described in the Materials and Methods. A and B show complexes between tau and SHP2; C and D show complexes between tau and activated SHP2 (act-SHP2). Tau was additionally labeled using anti-mouse IgG–Alexa Fluor 488. Nuclei were counter-stained with DAPI (inset and merge). Confocal projections are shown. Scale bar: 10 µm. (E) Quantification of tau–SHP2 (left) and tau–activated SHP2 (right) complexes found before and after NGF treatment (open and closed bars, respectively). For tau–SHP2 complexes, over 60 randomly chosen cells were evaluated; for tau-activated SHP2 complexes, over 100 randomly chosen cells were evaluated. After PLA puncta were counted, cells were then sorted into four groups according to the number of puncta they had (number of puncta as shown). The mean±s.d. from two independent experiments are shown. For tau–SHP2 complexes (left), the average numbers of PLA puncta in NGF-stimulated cells and non-stimulated cells were 20.1 and 11.9, respectively, which were significantly different when analyzed by Student's *t*-test (t=4.66, P=0.0431). (F) Quantification of pT231-tau–SHP2 complexes found before and after NGF treatment, shown from one representative experiment. Over 90 randomly chosen cells were evaluated. The mean numbers of PLA puncta in NGF-stimulated cells and non-stimulated cells were 79.6 and 47.4, respectively, which were significantly different when analyzed by Student's *t*-test ($P \leq 0.0001$). Data from three independent experiments indicated a 67% increase in the number of puncta from the PLA (P=0.0208) induced by NGF.

SHP2, the average ratio of PLA in processes:soma was 0.3 while for complexes of total tau and SHP2, the average ratio was 1.0 (Fig. 6F). This indicates that pT231 tau–SHP2 complexes are localized in the soma relative to processes at a ratio of approximately 10 to 3 whereas for total tau–SHP2 complexes, localization in the soma relative to processes are close to being equal.

Tau–SHP2 complexes were also examined in fixed brain tissues from 6-month-old WT mice. PLA, using DA9 and anti-SHP2 antibodies, was conducted on brain sections, with the control PLA omitting DA9. Endogenous tau–SHP2 complexes were observed in dentate gyrus, CA1 and cortex regions of the brain tissue (Fig. 6G), while no PLA signals were found in the control (Fig. 6H). Our data demonstrate the presence of tau–SHP2 complexes in adult mouse brains, suggesting that the complexes have a role in normal adult brain.

Tau–SHP2 complexes in human brain

AD brain has been shown to contain phosphoepitopes that are characteristic of developing systems, where the cells are still dividing (Bramblett et al., 1993; Goedert et al., 1993; Vincent et al., 1998). Given our observed increase of tau–SHP2 complexes upon NGF stimulation, there could be a role for the complex during neuronal development, raising the possibility that the tau–SHP2 complex could appear in AD brain. Since SHP2 has never been investigated in AD brain, post-mortem human hippocampal brain samples were first probed for SHP2; samples were obtained from control or patients with mild or severe AD (Table S1A). While control (NCI) sections had a very low level of SHP2 labeling, both mild (MCI) and severe AD sections showed more pronounced labeling (Fig. 7A) with some cells showing a higher level of SHP2 than neighboring cells (Fig. 7B). When double labeling with

Journal of Cell Science (2019) 132, jcs229054. doi:10.1242/jcs.229054

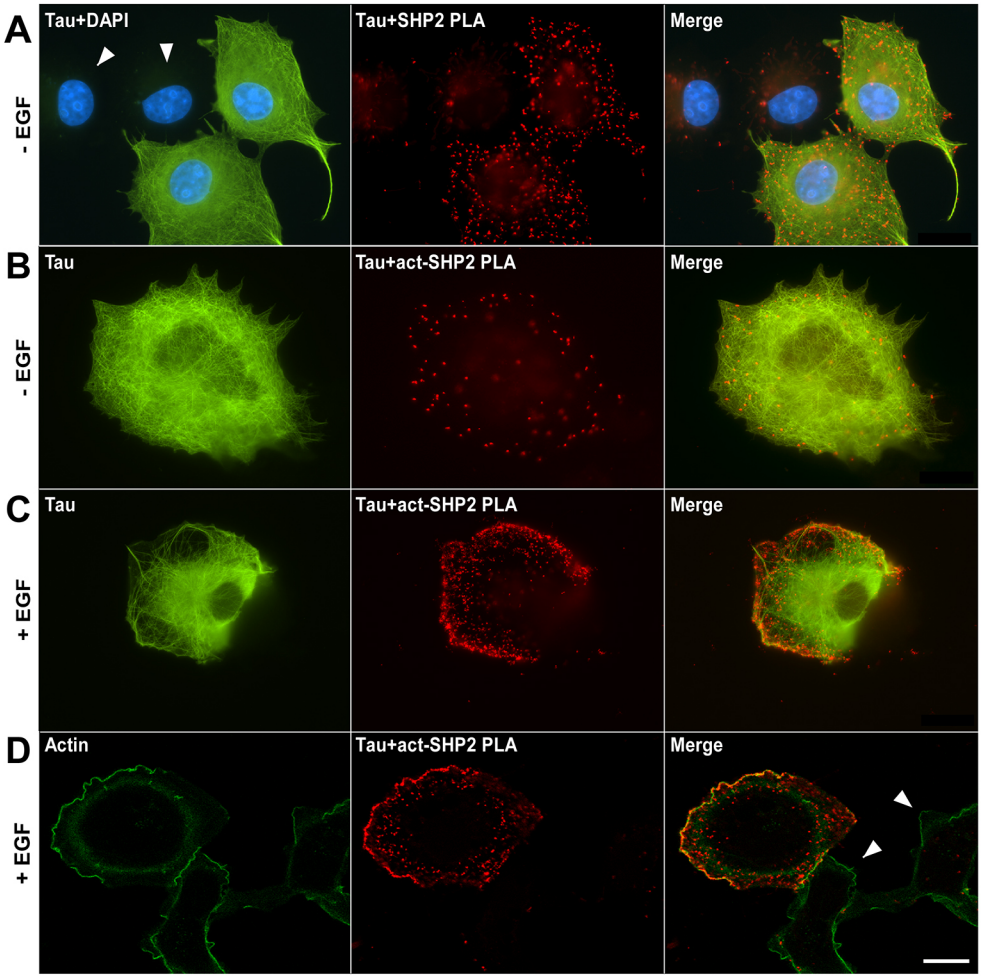

Fig. 4. Tau–activated-SHP2 complexes are localized to the membrane ruffles in COS7 cells. (A) COS7 cells expressing WT tau were subjected to PLA as described in the Materials and Methods using DA9 and anti-SHP2 antibodies. Tau was additionally labeled using anti-mouse IgG–Alexa Fluor 488. Nuclei were counter-stained with DAPI. Epifluorescence images were taken. (B,C) COS7 cells expressing WT tau were treated with (C) or without (B) EGF for 5 min. PLA was conducted using DA9 and anti-activated SHP2, and tau was additionally labeled using anti-mouse IgG–Alexa Fluor 488. Confocal projections are shown. (D) COS7 cells expressing WT tau were treated with EGF for 5 min. PLA was conducted using DA9 and anti-activated SHP2 antibodies. After conducting PLAs, actin filaments were stained with phalloidin–Alexa Fluor 488. Confocal projections are shown. Arrowheads indicate non-transfected COS7 cells. Scale bar: 10 µm.

immunofluorescent probes was used, SHP2 labeling often coincided with tau labeling in the severe AD cases (Fig. 7C, right column). In MCI, SHP2 labeling was less extensive, with colocalization still apparent in some areas (Fig. 7C, middle column). As a control, we confirmed that omitting anti-SHP2 abolished Alexa Fluor 488 labeling.

To identify tau–SHP2 complexes, hippocampal sections (Table S1B) were subjected to PLA, where antibodies against total tau and SHP2 were used; for reference, the tau signal was also visualized. PLA puncta were observed in the dentate gyrus, CA1, CA3 and subiculum regions (dentate gyrus and subiculum shown in Fig. 8A). Quantification of the puncta indicated that NCI samples had the least PLA puncta, with tau–SHP2 complexes significantly increasing in samples from patients with AD (Fig. 8B). While the subiculum had the highest level of puncta, the levels in the DG, CA3 and CA1 regions were not significantly different from one another (Fig. S2). Differences between the puncta level of MCI and severe AD cases was statistically significant only in the DG and subiculum regions (Fig. 8B).

DISCUSSION

We have shown that the association between tau and SHP2 was increased by phosphorylation at T231. Moreover, in cells responding to NGF, phosphorylation at T231 increased, with the association between tau and SHP2 increasing in a manner that required tau phosphorylation at T231. By using primary cultured neurons, we also found that complexes between SHP2 and tau that was phosphorylated at T231 favored a cell soma localization whereas complexes between SHP2 and tau, in general, were equally distributed between the cell soma and cell processes. Tau–SHP2 complexes were also found in brains from 6-month-old mice. Finally, while tau–SHP2 complexes were found at a low level in the control human brain, the level of tau–SHP2 complexes increased in MCI and severe AD brain, especially in the subiculum. The increase coincided with an increase of SHP2 labeling in MCI and severe AD. Our data demonstrate the importance of tau–SHP2 complexes in neuronal development and suggest a role for the complex in neurodegeneration.

In this study, the interaction between tau and SHP2 was initially demonstrated using biochemical approaches (co-IP and *in vitro* binding assays). However, by using PLA, a cell biological approach using fixed cells, it was possible to quantify the interaction and discern additional details. In conducting PLA on NGF-treated PC6-3 cells, the increased levels of tau-SHP2 complexes seen at the 5 min time point indicated that NGF-stimulated phosphorylation changes were the likely cause. By using T231D and T231A tau mutants, our PLA data suggest that the NGF-induced increase in pT231 is required for the increase in tau–SHP2 complexes. The use of PLA to examine the association was vital since, on a biochemical level using co-IP conditions, while we were able to immunoprecipitate pT231 tau from non-stimulated PC6-3, we were unable to immunoprecipitate pT231 tau from NGF-stimulated PC6-3 cells. In contrast, by performing immunoprecipitates using a RIPA buffer for solubilization or by flow cytometry, we had found that pT231-tau increased following NGF stimulation (Leugers and Lee, 2010). This indicated that in response

Journal of Cell Science (2019) 132, jcs229054. doi:10.1242/jcs.229054

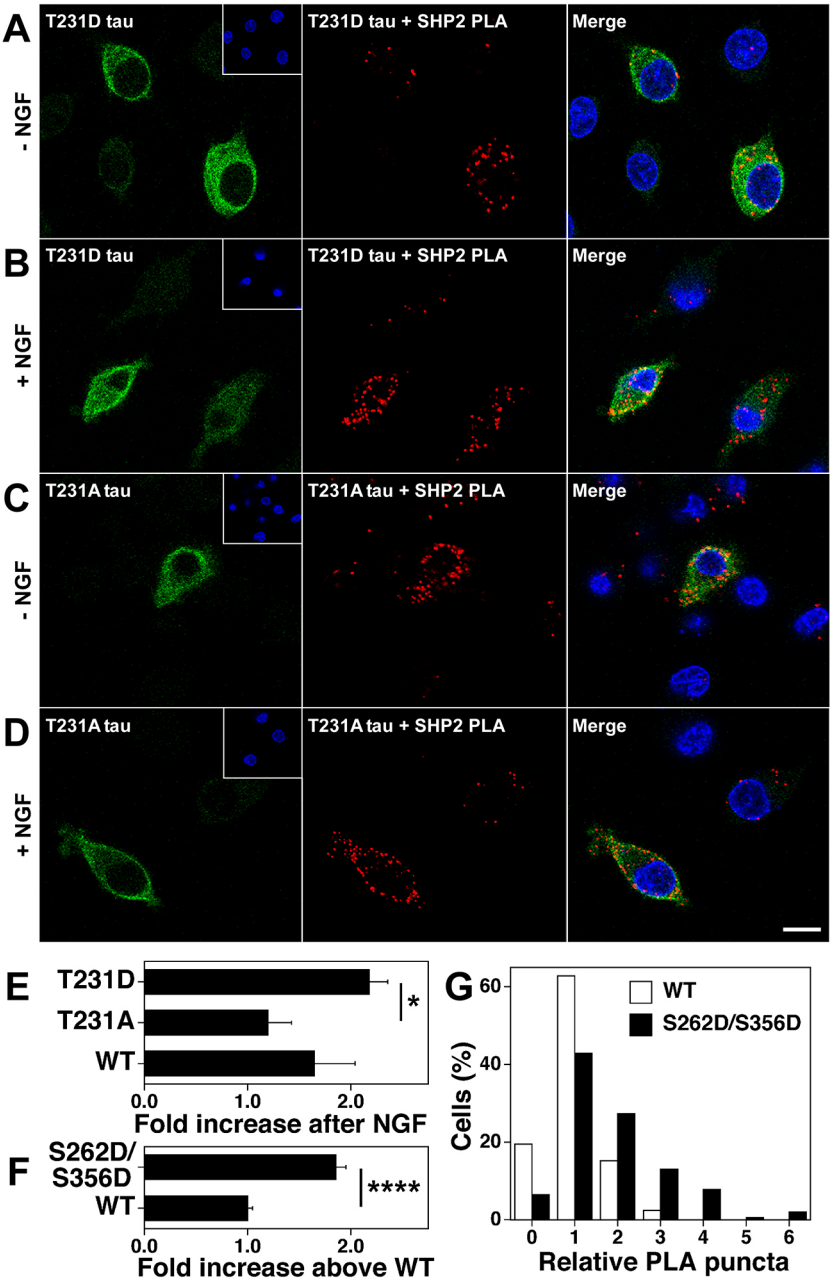

Fig. 5. Phosphorylation at T231 of tau is required for the NGF-induced increase in the SHP2 association. (A–D) rTau4 cells expressing T231D tau (A,B) or T231A tau (C,D) were treated with or without NGF for 3 h. PLAs were then conducted using DA9 and anti-SHP2, with tau being additionally labeled using anti-mouse IgG-Alexa Fluor 488. Nuclei were counter-stained with DAPI (inset and merge). Confocal projections are shown. Scale bar: 10 µm. (E) For each well, 70–90 transfected cells were randomly selected. For each cell, using a confocal microscope, the optical section containing the most PLA puncta was analyzed. PLA signals were quantified and normalized as described in the Materials and Methods. The NGF-induced fold increase in the PLA signals for each construct was calculated by determining the ratio of the signals of with NGF to without NGF. The fold increases exhibited by WT, T231D, and T231A tau were statistically compared with an ANOVA test: WT versus T231D, P=0.2096; WT versus T231A, P=0.2338; T231D versus T231A, P=0.0332 (*P<0.05). Results are mean±s.e.m. from three independent experiments. (F) rTau4 cells expressing WT or S262D/S356D tau were subjected to PLA as described in A. PLA signals were quantified and normalized as described in the Materials and Methods, comparing S262D/S356D tau to WT. Fold increase exhibited by S262D/S356D tau relative to WT was statistically significant, as compared by Student's t-test (****P<0.0001). Results are mean±s.e.m. from four independent experiments. (G) Distribution of relative WT tau–SHP2 and S262D/S356D tau–SHP2 PLA values evaluated in panel F. A total of 164 WT and 154 S262D/S356D transfected cells were analyzed.

to NGF, pT231-tau shifts its cellular localization such that it cannot be solubilized by a co-IP lysis buffer. Therefore, if one were using co-IPs, there would be a population of tau–SHP2 complexes that would not be detected. PLA allowed us to detect tau–SHP2 complexes in fixed cells and to document an increase in tau–SHP2 complexes following growth factor stimulation.

When visualizing the cellular location of tau–SHP2 complexes in PC6-3 cells, it was difficult to ascertain changes following NGF addition. However, in EGF-stimulated COS7 cells, tau–SHP2 complexes appeared to localize at the actin ruffles on the plasma membrane. Given that tau also associated with activated SHP2 (Figs 3 and 4), we speculate that following NGF stimulation of PC6-3 cells, tau–SHP2 complexes are located in lipid rafts. Tau has been reported to reside in lipid rafts (Hernandez et al., 2009; Kawarabayashi et al., 2004; Klein et al., 2002) and lipid raft-associated SHP2 appears to be involved in integrin-mediated signaling and growth factor receptor signaling pathways (Bryant et al., 2009; Lacalle et al., 2002). A lipid raft localization for tau–SHP2 complexes would also explain our inability to solubilize the complex with standard co-IP buffer. With the importance of lipid rafts in signaling, these observations would suggest a role for tau–SHP2 complexes in NGF signaling. We have previously shown that tau has a critical role in NGF signaling where tau affected MAPK activation without needing to interact with microtubules (Leugers and Lee, 2010). The role of the tau–SHP2 association in this pathway remains to be investigated. It will be important to establish the temporal order of appearance and disappearance for pT231 and pY18 following NGF addition, where tau in the soluble as well as insoluble compartments is examined.

The importance of tau–SHP2 complexes in neuronal cells was also demonstrated by our identification of such complexes in primary hippocampal neurons. The presence of such complexes in the cell soma as well as in neuronal processes indicates that tau–SHP2 complexes may function in more than one signaling pathway

Journal of Cell Science (2019) 132, jcs229054. doi:10.1242/jcs.229054

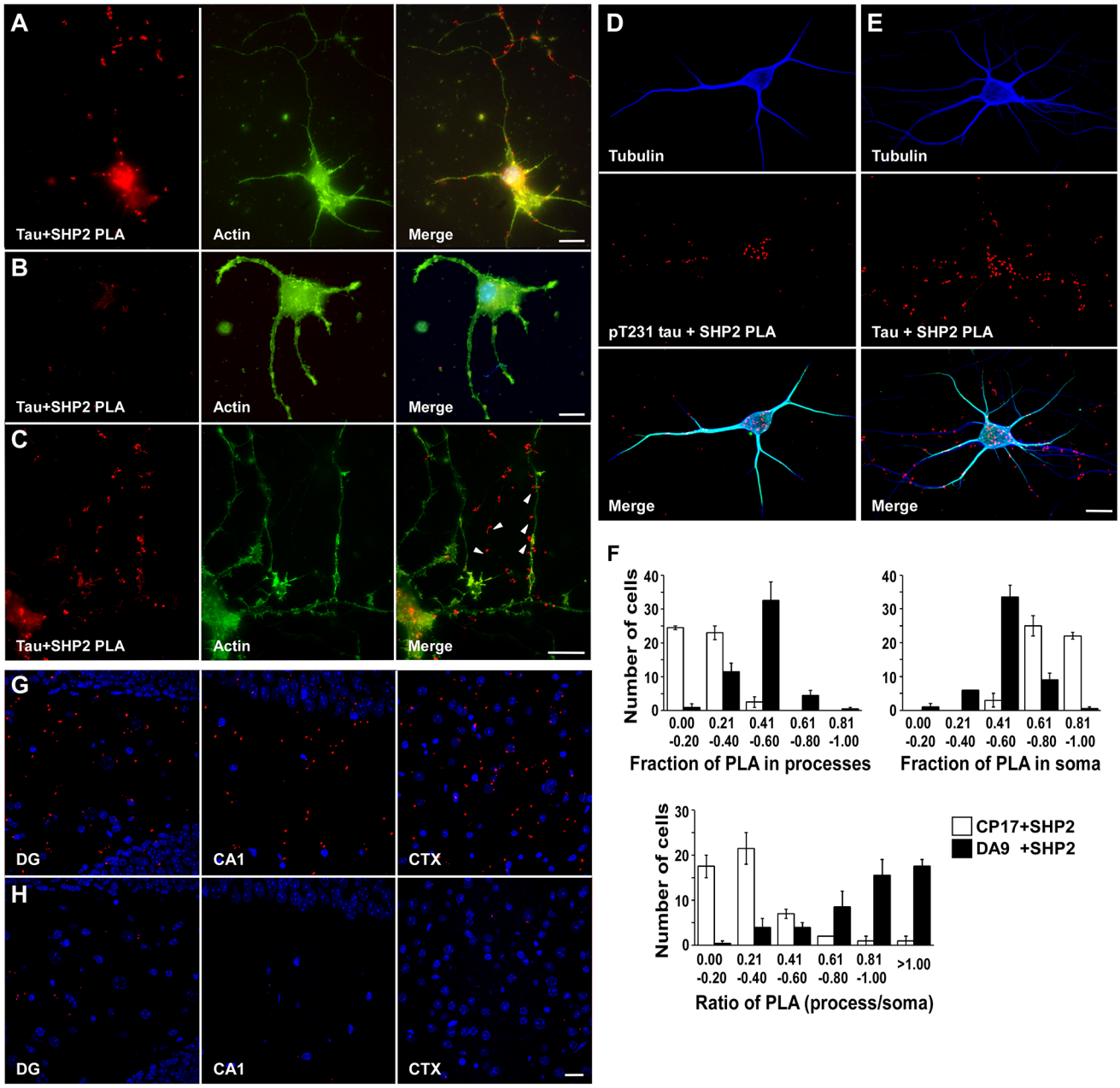

Fig. 6. Tau and SHP2 complexes are present in primary hippocampal neurons and in adult mouse brain. (A,B) Hippocampal neurons from WT (A) or tau-knockout (B) mice were subjected to PLAs using DA9 and rabbit anti-SHP2 antibodies as described in the Materials and Methods. Actin was labeled with phalloidin–Alexa Fluor 488. Epifluorescence images were taken. (C) As seen at a higher magnification, PLA puncta in WT mice appeared to lie adjacent to neuronal processes. Arrowheads indicate examples of PLA puncta that lie next to neuronal processes. (D,E) To visualize the association between SHP2 and pT231 tau or total tau in primary neurons, PLAs were performed using rabbit anti-SHP2 and CP17 (recognizing pT231 tau; D) or DA9 (for total tau; E) antibodies. Tubulin was labeled using rat anti-tubulin and donkey anti-rat IgG–AMCA antibodies. MAP2 was labeled using chicken anti-MAP2 and donkey anti-chicken-IgG–Alexa Fluor 488. Confocal projections are shown. (F) Fifty neurons were randomly chosen and the PLA puncta from both soma and processes were counted. For each cell, the proportion of puncta in processes, the proportion of puncta in soma, and the ratio of puncta in the processes over soma were calculated, and are shown in the graphs. Results are mean±s.d. from two independent experiments. (G,H) Brain sections of WT mouse were subjected to PLA, using DA9 and rabbit anti-SHP2 antibodies (G) or only rabbit anti-SHP2 antibody as a control (H). Nuclei were counterstained with DAPI. Dentate gyrus (DG), CA1, and cerebral cortex (CTX) were examined. Confocal projections are shown. Scale bars: 10 µm (for A–E), 20 µm (for G,H).

in neurons. The interaction between phosphorylated tyrosine residues and an SH2 domain of SHP2 activates SHP2 activity (Sugimoto et al., 1994), and the possibility that tau may regulate SHP2 activity remains to be investigated. The role of T231 in the interaction may be indirect, as phosphorylation at T231 could lead to unfolding of tau, rendering other regions accessible for interaction with SHP2. Additionally, phosphorylation at T231 reduces the association of tau to microtubules, and our data would suggest that a reduction in microtubule association promotes SHP2 association (Fig. 5F,G). Our finding that, in primary hippocampal neurons, the localization of pT231-tau–SHP2 complexes differed from that of total tau–SHP2 complexes may result from several possibilities. While we have found that the distribution of pT231-tau relative to total tau supported the differential localization

Journal of Cell Science (2019) 132, jcs229054. doi:10.1242/jcs.229054

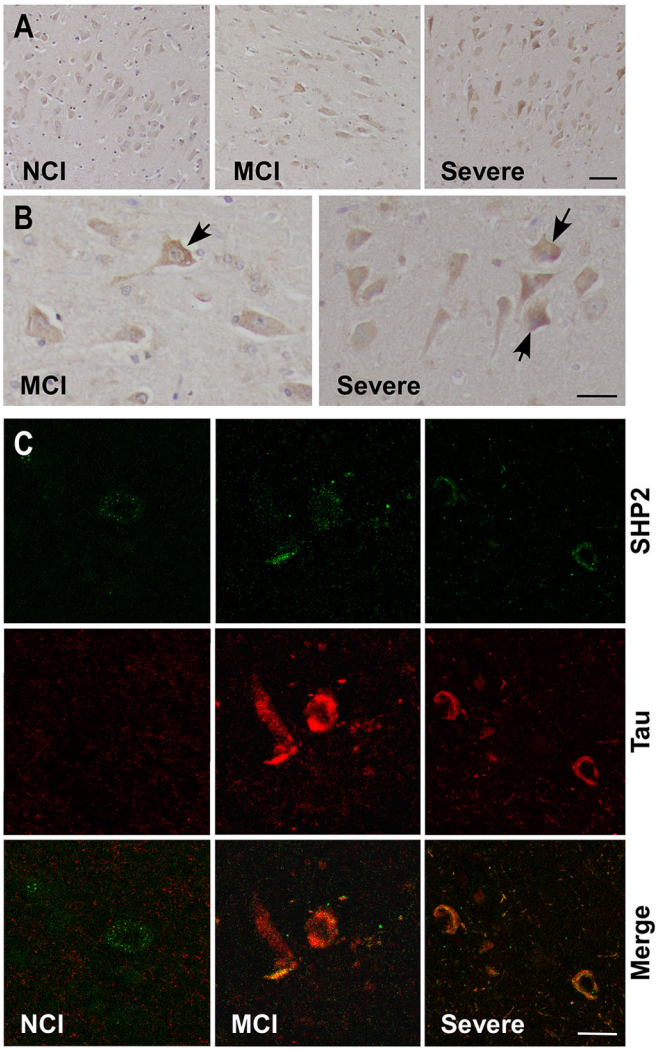

Fig. 7. MCI and brain sections from patients with severe AD contain more SHP2 than control brains. (A) Hippocampal sections of post-mortem human brains were labeled immunohistochemically with anti-SHP2 as described in the Materials and Methods. NCI, control; MCI, mild AD; severe, severe AD. Scale bar: 80 µm. (B) Hippocampal sections of post-mortem human brains from MCI (left) or severe (right) AD patients were labeled immunohistochemically with anti-SHP2 antibody as described in the Materials and Methods; arrows indicate cells with higher levels of SHP2. Scale bar: 40 µm. (C) Hippocampal sections of post-mortem human brains (NCI, MCI or severe AD patients) were double-labeled with anti-SHP2 (top) and DA9 (middle) antibody and processed for immunofluorescence labeling as described in the Materials and Methods. Merged images (bottom) show colocalization of SHP2 and tau being more extensive in severe AD sections. Scale bar: 20 µm.

of pT231-tau–SHP2 complexes (Fig. S3), other explanations contributing to the distribution of the PLA signals cannot be ruled out. The ability of PLA to identify complexes that differ with respect to tau phosphorylation enlarges the types of questions that can be asked and answered. In addition, our localization of tau–SHP2 complexes in adult mouse brain indicated a role for the interaction beyond developing systems, and also demonstrated the feasibility of performing PLA on fixed tissue sections.

In examining pY18 tau as a substrate for SHP2, we found that tau served as a substrate for SHP2 *in vitro* (Fig. 2). However, since the commercially obtained SHP2 lacked its N-terminus, whether tau serves as a substrate for SHP2 in cells remains to be determined. Phosphorylation of tau at Y18 takes place during early brain development but disappears by postnatal day 21 (Lee et al., 2004), despite Fyn activity being maintained up to postnatal day 35 (Inomata et al., 1994), suggesting that pY18 tau may be dephosphorylated during development.

Developmental events, such as phosphorylation of tau on mitotic epitopes during neuronal cell division, have been associated with AD (reviewed in Raina et al., 2004). Given our finding that the tau–SHP2 complex is present in a developing neuronal system, we investigated the possibility that the tau–SHP2 complex might be present in AD samples. SHP2 has not been associated with AD, although activated SHP2 has been linked to various cancers (reviewed in Zhang et al., 2015), and this may be relevant to the idea that AD is a form of cancer where there is a loss of cell cycle control (reviewed by Herrup and Yang, 2001; Nagy, 2000; Wang et al., 2009; Webber et al., 2005). Our finding that MCI and severe AD brain sections contained increased levels of SHP2 relative to control brain indicate that SHP2 is upregulated during AD. In addition, our findings indicate that while the tau–SHP2 association occurred in normal adult brain, its level significantly increased during MCI and severe AD. While the pattern of PLA puncta and its relationship to tau pathology remain to be investigated, the ability to obtain evidence for a protein complex in post-mortem human brain provides a new detection tool for disease mechanisms. Since the PLA protocol uses an amplification step, it is able to mark regions where an interaction between two proteins has occurred. Given our previous findings on the appearance of pY18 tau in AD brain (Lee et al., 2004), our findings allow us to speculate that SHP2 may be acting on/with tau during neurodegeneration.

Together with our data, the critical role of SHP2 during neuronal development (Wright et al., 1997) suggests that tau–SHP2 complexes might promote MAPK activation. Activated MAPK has been found in AD cases (Pei et al., 2002), and since an abnormal increase in MAPK signaling during AD could drive abnormal cell cycle activation (reviewed in Zhu et al., 2002), one would speculate that the tau–SHP2 complex would promote cell cycle re-entry. Phosphorylation at Y18 of tau has been found to be required for amyloid β (Aβ)-induced cell cycle re-entry, since the Y18F mutant tau fails to promote Aβ-induced cell cycle re-entry (Seward et al., 2013). This raises the possibility that phosphorylation at Y18 of tau may increase its interaction with SHP2 and activate SHP2, driving cell cycle re-entry. Such a possibility remains to be investigated. Finally, the report that SHP2 associates with Grb2-associated-binding protein 2 (Gab2) (Gu et al., 1998) may also be relevant for AD since *GAB2* has been identified as a gene whose variants correlated with increased susceptibility to late-onset AD (Hu et al., 2017; Reiman et al., 2007).

In conclusion, the presence of tau–SHP2 complexes in a neuronal cell line, primary neuronal culture and in adult brain indicates that the interaction has long-lived cellular function. Given that phosphorylation of tau at T231 promotes the association, the presence of pT231 tau in samples from patients with mild AD suggests that tau–SHP2 complexes might occur during the early stages of neurodegeneration. Our finding of tau–SHP2 complexes in both mild and severe AD cases supports this prediction and suggests that the tau–SHP2 association has a role during neurodegeneration. Finally, since tyrosine phosphorylation is used to regulate signal transduction mechanisms, the association between tau and SHP2 suggests that tau has a function in signal transduction.

MATERIALS AND METHODS

Cell culture

The cell types used in this study were COS7, PC6-3 (Pittman et al., 1993), and two cell lines derived from PC6-3 (D5 and rTau4; Leugers and Lee,

Journal of Cell Science (2019) 132, jcs229054. doi:10.1242/jcs.229054

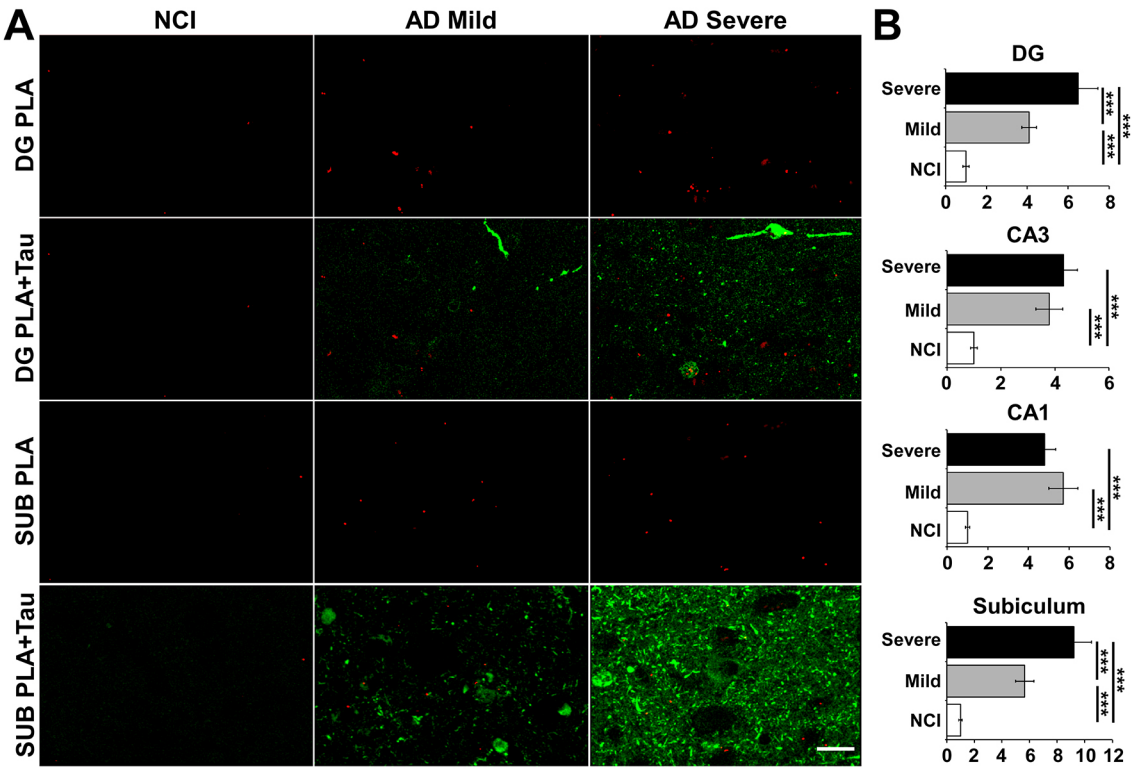

Fig. 8. AD-affected brains contain more complexes of tau and SHP2, relative to non-diseased brains. (A) Hippocampal sections of post-mortem human brains (NCI, MCI or severe AD patients) were subjected to PLA using DA9 and rabbit anti-SHP2 antibodies as described in the Materials and Methods. Tau was additionally labeled using anti-mouse IgG–Alexa Fluor 488. Confocal projections are shown. Representative images show the PLA puncta and the PLA+tau merged signals in dentate gyrus (DG) and subiculum (SUB) of NCI, MCI, or severe AD samples. Scale bar: 20 µm. (B) Quantification of the relative number of PLA puncta in DG, CA3, CA1, or subiculum region from six NCI, six MCI, and six severe AD patients. For each patient, PLA puncta were counted from 10 randomly selected areas of each region. For each region, to compare the amount of PLA between the patient groups, all the counted PLA puncta were normalized to the average of PLA puncta in NCI control, and are presented relative to the NCI value (set as 1). The averages of the normalized PLA puncta were then statistically compared by performing one-way ANOVA for each region, followed by the honest significant difference post-hoc test. Results are mean± s.e.m. (***P<0.001).

2010). COS7 and PC6-3 cells have not been reported as contaminated or misidentified (International Cell Line Authentication Committee, October 14, 2018). COS7 cells were maintained in DMEM with 10% fetal bovine serum (Hyclone). PC6-3 cells were grown on collagen (BD Biosciences)-coated flasks in RPMI 1640 medium with 10% horse serum and 5% fetal bovine serum (Hyclone); D5 and rTau4 cells were cultured in the same medium supplemented with 200 µg/ml of G418 (Leugers and Lee, 2010).

Animals

Animal care was in compliance with National Institutes of Health guidelines for the care and use of laboratory animals. All animal procedures were approved by the University of Iowa Institutional Animal Care and Use Committee.

Human AD samples – ethics approval, consent to participate and consent for publication

Post-mortem brain tissues were obtained from 23 human participants. For post-mortem human samples obtained from the autopsy service at the University of Iowa, the study was determined to be exempt from review by University of Iowa Institution Review Board; ethics approval and consent were waived. For post-mortem human samples obtained from Rush Alzheimer's Disease Center, subjects signed an informed consent and Anatomical Gift Act. All clinical investigations have been conducted according to the principles expressed in the Declaration of Helsinki.

Primary mouse hippocampal neuronal culture

WT mice or homozygous tau-knockout mice (Dawson et al., 2001) were obtained from The Jackson Laboratory (C57Bl/6 strain). Primary hippocampal neuronal cultures were prepared from newborn [postnatal day (P)0] mouse pups as previously described (Beaudoin et al., 2012). All animal experiments were performed according to approved guidelines, as described above in 'Animals'. Briefly, hippocampus from P0 pups were isolated in Neurobasal A medium (Gibco, 10888-022) containing 0.5 mM glutamine, 1% penicillin/streptomycin and 10 mM HEPES, chopped into fine pieces and digested in 1 mg/ml trypsin (Sigma, T7409) for 10 min at 25°C. Tissues were washed twice and resuspended in Neurobasal A medium. The tissues were then triturated three times with three pasteur pipettes, each with a narrower opening than the previous one. After this, MEM with 2% horse serum and 6 µM insulin (Sigma, I5500) was added, and 300 µl of the cell suspension was layered onto coverslips that had been treated with 0.2 mg/ml poly-L-ornithine and 0.05 mg/ml laminin. After incubating the coverslips for 3 h at 37°C and 5% CO_2, 1 ml Neurobasal A medium containing 20 µl B27 (Gibco, 17504044) was added to each coverslip.

Plasmid constructions and recombinant proteins

0N3R human tau (the 352 residue isoform, hereafter 3R tau) was expressed in eukaryotic cells using pRc/CMV n123c plasmid as previously described (Hall et al., 1997). The tau mutant T231A tau was generated by site-directed mutagenesis (QuikChange Mutagenesis Kit, Stratagene) using pRc/CMV n123c as template; the mutation was confirmed by DNA sequencing. The pRc/CMV plasmid expressing the 3R tau mutant T231D has been previously described (Sharma et al., 2007).

For recombinant tau proteins, bacterial expression pET constructs encoding 3R WT and T231D mutant tau have been previously described (Bhaskar et al., 2005; Brandt and Lee, 1993). Proteins were expressed in BL21(LysS)DE3 *E. coli* cells and purified as previously described (Bhaskar et al., 2005; Brandt and Lee, 1993).

Journal of Cell Science (2019) 132, jcs229054. doi:10.1242/jcs.229054

Cell transfection and preparation of lysates

COS7 cells were plated on 100 mm dishes and transfected with tau plasmids using Lipofectamine 2000 as recommended by the manufacturer (Invitrogen). PC6-3 cells stably expressing 3R tau (D5) were plated on collagen-coated 150 mm dishes and serum starved overnight prior to growth factor treatment (50 ng/ml NGF; N2513 Sigma). Cell lysates were prepared as previously described (Leugers and Lee, 2010; Sarkar et al., 2008). Briefly, COS7 cells from each plate were harvested 48 h after transfection, using 1 ml of ice-cold lysis buffer containing 50 mM Tris-HCl pH 7.5, 150 mM NaCl, 1% Triton X-100, 0.25% deoxycholate, 1 mM EDTA, 1 mM EGTA, 1 mM sodium vanadate, 10 mM sodium fluoride, 1 mM AEBSF, 2.16 mM leupeptin, 1.46 mM pepstatin and 0.15 mM aprotinin. D5 cells were harvested with 1 ml of the same lysis buffer. Following 30 min incubation with gentle mixing at 4°C, lysates were cleared by centrifugation at 6200 ***g*** for 20 min at 4°C.

Co-immunoprecipitation and immunoblotting

Cleared cell lysates were incubated with 1.5 µg non-specific IgG (Jackson ImmunoResearch) at 4°C for at least 4–16 h, followed by an additional incubation for 1 h with protein A–Sepharose (GE Healthcare) or protein G–Sepharose (EMD Millipore). Following centrifugation (16,000 ***g*** for 1 min), the resulting pre-cleared supernatants from COS7 or D5 cells were incubated with DA9 [100 µl mouse monoclonal supernatant against total tau, generously provided by Dr Peter Davies, Litwin-Zucker Center for Alzheimer's Disease and Memory Disorders, Feinstein Institute for Medical Research, NY, USA (Tremblay et al., 2010)], rabbit polyclonal anti-SHP2 (1.5 µg, sc-280, Santa Cruz Biotechnology) or CP17 [3.5 µg, mouse monoclonal anti-pT231 tau, generously provided by Dr Peter Davies (Weaver et al., 2000)] overnight at 4°C. Lysates were incubated with protein A– or protein G–Sepharose for an additional 1 h. After washing, immunoprecipitates were run on SDS-PAGE gels (7.5 or 12% acrylamide) and transferred onto Immobilon-P PVDF membranes (Millipore). Blots were blocked using 2 or 4% BSA in Tris-buffered saline containing 0.05% (v/v) Tween-20 (TBS-T). Blots were incubated with primary antibodies overnight at 4°C or for 1.5–2 h at room temperature, followed by incubation with horseradish peroxidase (HRP)-conjugated secondary antibodies (Jackson ImmunoResearch). Blots were developed with Amersham ECL Plus reagent (GE Healthcare). Primary antibodies used were: Tau13 (0.5 µg/ml, mouse monoclonal against human tau, generously provided by the late Dr Lester Binder), rabbit polyclonal anti-SHP2 antibody (0.4 µg/ml, sc-280, Santa Cruz Biotechnology), mouse monoclonal anti-paxillin antibody (0.05 µg/ml, 05-417, Upstate Biotechnology) or 9G3 (1 µg/ml, mouse monoclonal against pY18 tau; Lee et al., 2004). Tau5–HRP antibody (1:50,000; Leugers and Lee, 2010) was also used.

In vitro binding assays

COS7 cells were plated on 100 mm dishes and harvested in 1 ml of ice-cold lysis buffer containing 50 mM Tris-HCl pH 7.5, 150 mM NaCl, 2% Nonidet P-40 (NP-40), 1 mM EDTA, 1 mM EGTA, 1 mM sodium vanadate, 10 mM sodium fluoride, 1 mM AEBSF, 2.16 mM leupeptin, 1.46 mM pepstatin and 0.15 mM aprotinin. Lysates were cleared by centrifugation at 6200 ***g*** for 20 min at 4°C. SHP2 or paxillin was immunoprecipitated as described above using rabbit polyclonal anti-SHP2 antibody (1 µg, sc-280, Santa Cruz Biotechnology) or mouse monoclonal anti-paxillin antibody (1 µg, 05-417, Upstate Biotechnology). After washing, recombinant tau proteins (0.5 µg) were added to the immunoprecipitated SHP2 (or paxillin) in a reaction buffer containing 50 mM HEPES pH 7.4, 2 mM EDTA, 5 mM 2-mercaptoethanol (Sigma), 100 mM NaCl, 1 mM sodium vanadate, 10 mM sodium fluoride, 1 mM AEBSF, 2.16 mM leupeptin, 1.46 mM pepstatin and 0.15 mM aprotinin. After incubation at 4°C for 1.5 h, the resulting protein complexes were washed five times, resolved by SDS-PAGE and analyzed by immunoblotting.

SHP2 assays

To assay the activity of SHP2 on full-length tau *in vitro*, tyrosine phosphorylated tau was prepared by adding Fyn tyrosine kinase (14-441, Millipore) to *E. coli*-synthesized 3R tau (352 residue isoform), as previously described (Lee et al., 2004). Briefly, 1 µg of *E. coli*-synthesized tau was incubated with Fyn (4 U) in kinase reaction buffer (100 mM Tris-HCl pH 7.2, 25 mM $MnCl_2$, 2 mM EGTA, 2 mM DTT, 242 µM ATP, 31.5 mM $MgCl_2$) for 2 h at 37°C. The reaction buffer was then converted into phosphatase buffer containing 10 µM PP2 (172889-27-9, Millipore), 2 mM 2-mercaptoethanol and 5 mM EDTA. Then, 0.36 µg SHP2 (SRP0217, Sigma) was added and reactions were incubated for 1 h at room temperature. Control phosphatase reactions omitted SHP2. To analyze tyrosine phosphorylation, reactions were resolved by SDS-PAGE, followed by immunoblotting using 9G3 to detect pY18 tau.

To assay the activity of SHP2 on a tyrosine phosphorylated tau peptide, a 96-well plate was coated with NeutrAvidin as previously described (Jicha et al., 1997), and then blocked with 2% BSA, 1 h at 25°C. 0.005 µM biotinylated-pY18 tau peptide (Biotin-EDHAGTpYGLGDRK; residues 12–24) was incubated with 0.8 µg SHP2 (Sigma) in a reaction buffer containing 50 mM HEPES pH 7.4, 0.5 µg BSA and 1 mM DTT for 1 h at 25°C. The control reactions either used biotinylated non-pY18 tau peptide or boiled SHP2 (5 min at 95°C). Omitting SHP2 in each reaction was also included as a negative control. To determine the background levels, 2% BSA instead of pY18 tau peptide was used. To assess phosphorylation at Y18, biotinylated peptides were first captured by adding the reactions to the NeutrAvidin-coated plate and incubating for 1 h at 25°C. After washing with TBS, 9G3 (anti-pY18 tau, 1:60 dilution) was added and incubated for 2 h at 25°C. Background level was determined by omitting 9G3. After washing with TBS-T, the plate was incubated with HRP-conjugated donkey anti-mouse IgG (Jackson Immuno Research, 1:2000) for 2 h at 25°C. After washing with TBS-T, plates were developed with the Bio-Rad ABTS peroxidase substrate. Optical density was measured at 405 nm using an SLT Spectra plate reader (Tecan Technicals).

In situ PLAs

PLAs are designed to detect protein–protein interaction *in situ* (Gustafsdottir et al., 2005; Söderberg et al., 2006). In the assay, the two proteins are labeled with primary antibodies raised in different species, which are then detected by secondary antibodies that are differentially labeled with specific oligonucleotides. With added components, association of the two proteins, as defined by the secondary antibodies lying within 40 nm of each other, allows for rolling circle amplification. The rolling circle product is then specifically detected by a fluorescent oligonucleotide probe. PLA components were purchased from Sigma (Duolink® *in situ*).

To perform PLA on COS7, PC6-3 or rTau4 cells, COS7 cells were seeded onto 12 mm glass coverslips and PC6-3 or rTau4 cells were seeded onto collagen-coated chamber slides (Lab-Tek Permanox, 177437, Thermo Fisher Scientific). COS7 or rTau4 cells were transfected using Lipofectamine 2000 as recommended by the manufacturer (Invitrogen). For P0 primary hippocampal culture, the cells, seeded on poly-L-ornithine and laminin-treated coverslips, were grown for an additional 5 or 10 days. All cells were fixed with 0.3% glutaraldehyde as previously described (Lee and Rook, 1992) except with the use of 0.1% saponin instead of 0.5% NP-40. Primary antibodies used were mouse monoclonal antibody supernatant against total tau DA9 (1:50), mouse monoclonal anti-pT231 tau (CP17, 1.7 µg/ml) and rabbit polyclonal anti-SHP2 (sc-280, Santa Cruz Biotechnology, 1 µg/ml). Following the manufacturer's protocol, secondary antibodies (anti-rabbit PLUS probe and anti-mouse MINUS probe, Sigma) were incubated with the cells, and following the Duolink protocol, if the two proteins were sufficiently close, rolling circle amplification was triggered by the subsequent additions. Amplified DNA was detected by a specific oligonucleotide that was labeled with an orange fluorophore (λ_{ex} 554 nm; λ_{em} 579 nm). For primary hippocampal cultures, after conducting PLA, anti-tubulin (rat monoclonal supernatant YL1/2, YSRTMCA77S, Accurate Chemical, 1:50) and chicken polyclonal anti-MAP2 (PA1-10005, Thermo Fisher Scientific, 1:2000), were added and incubated overnight at 4°C; donkey anti-rat IgG conjugated to AMCA and donkey anti-chicken IgG conjugated to Alexa Fluor 488 secondary antibodies were used to visualize tubulin and MAP2, respectively. To visualize total tau (DA9) in cell lines, incubation with goat anti-mouse IgG conjugated to Alexa Fluor 488 secondary antibody was added as a final step. To label actin cytoskeletons of primary neurons, phalloidin–Alexa Fluor 488 (8878, Cell Signaling Technology) was used. Cells were analyzed via epifluorescence microscopy (Nikon E800 microscope) or confocal microscopy (Zeiss 710

Journal of Cell Science (2019) 132, jcs229054. doi:10.1242/jcs.229054

confocal microscope). To analyze PLA signals in primary neurons, 50 cells were randomly selected from each well and the PLA puncta on neuronal processes and cell soma of each cell were counted.

For growth factor-stimulated cells, PLAs were performed on seeded cells that had been serum starved overnight and incubated with growth factor for 5 min [50 ng/ml NGF (N2513, Sigma) for PC6-3 and transfected rTau4 cells; 10 ng/ml EGF (RDI-115, Research Diagnostics) for transfected COS7 cells]. To assay the association between tau and activated SHP2, PLAs were performed using DA9 (1:50) and anti-activated SHP2 (rabbit monoclonal supernatant, ab62322, Abcam, 1:10,000). The association between tau and total SHP2 was assessed as described above. To analyze PLA signals in PC6-3 cells, the PLA puncta were counted on 60 randomly selected cells. To assay the association between pT231-tau and SHP2, PLAs were performed using CP17 (1.7 µg/ml) and anti-SHP2 (rabbit polyclonal, sc-280, Santa Cruz Biotechnology, 1 µg/ml). Analysis was carried out as described for DA9-labeled PC6-3 cells.

For assessing the effect of phosphorylation at T231 of tau, PLAs were performed on 3 h NGF-treated rTau4 cells expressing WT, T231D or T231A tau, using DA9 and anti-SHP2. To quantify the change in PLA puncta between non-stimulated and NGF-stimulated rTau4 cells that expressed WT, T231D or T231A, 70–90 transfected cells from each culture were randomly chosen. Then, using a Zeiss 710 confocal microscope, an optical section of each cell showing the most PLA signals was imaged; the tau signal was also captured. ImageJ was then used to determine the tau signal intensity for each cell and the PLA signal for each cell was quantified after thresholding (all cells in each experiment were subject to the same thresholding conditions). For each cell, the thresholded PLA signal was then normalized by dividing the PLA signal by the tau signal, thus eliminating the effect of different expression levels of tau on the extent of SHP2 association. Following this procedure, for each tau construct, average PLA signals were obtained for non-stimulated and NGF-stimulated cells, and the NGF-induced change was then calculated by dividing the NGF PLA signal by the PLA signal from non-NGF-treated cells. For testing the effect of the loss of microtubule binding, a similar experiment was performed using the S262D/S356D mutant of tau, without the use of NGF. For each experiment, relative PLA was calculated after (1) the PLA signal from each cell was normalized with respect to the tau level and (2) after normalization, the average relative PLA level for WT cells was set to '1' and S262D/S356D levels presented as a change relative to the '1' value. This calculation allowed comparison of the four experiments. A total of 164 WT and 154 S262D/S356D transfected cells was analyzed.

Brain sections

Paraffin-embedded brain sections prepared from 6-month-old WT or tau-knockout mice (Dawson et al., 2001) were deparaffinized and subjected to antigen retrieval (De Borst et al., 2007). The sections were then blocked for 1 h at room temperature with a blocking solution containing 5% normal goat serum, 3% BSA, 0.3% Triton X-100 (Fluka) in 1× PBS. Incubation with primary antibodies using the same blocking solution was conducted overnight at 4°C. Primary antibodies used were: DA9 (1:50) and rabbit polyclonal anti-SHP2 (1 µg/ml, sc-280, Santa Cruz Biotechnology). PLAs were performed as described above. Images of dentate gyrus, hippocampus and cerebral cortex were taken with a Zeiss 710 confocal microscope.

For examining human material by immunohistochemical staining, control, mild, and severe AD hippocampal brain samples were obtained from the University of Iowa Health Care System. For post-mortem human brain samples obtained from the autopsy service at the University of Iowa, our study was determined to be exempt from review by the University of Iowa Institutional Review Board; ethics approval and consent were waived. Braak staging, Thal, and CERAD scores for each case are shown in Table S1A. Paraffin-embedded sections were deparaffinized, subjected to antigen retrieval, and labeled with rabbit polyclonal anti-SHP2 (0.2 µg/ml, sc-280, Santa Cruz Biotechnology), HRP-coupled anti-rabbit-IgG (Dako EnVision), DAB and Dako Enhancer. Microscopy was performed with an Olympus BX61.

For immunofluorescence staining and PLA assays, paraffin-embedded human hippocampal brain sections of non-cognitive impairment (NCI), mild AD (MCI), and severe AD patients were obtained from Rush Alzheimer's Disease Center at Rush University Medical Center. Braak staging scores, neurofibrillary tangles assessments, and COGDX scores for each case are shown in Table S1B. For double immunofluorescence staining, human hippocampal brain sections were deparaffinized, blocked as above, and labeled with DA9 (1:50) or 9G3 (1:1000) and rabbit polyclonal anti-SHP2 (0.2 µg/ml, sc-280, Santa Cruz Biotechnology). Anti-rabbit-IgG conjugated to Alexa Fluor 488 and anti-mouse-IgG conjugated to rhodamine were used as secondary antibodies. Sections were analyzed by confocal microscopy (Leica SP8 STED). Three subjects for each type were labeled and representative images shown. For analysis by PLA, as described above, the sections were deparaffinized, blocked, and subjected to PLA. After labeling total tau with goat anti-mouse IgG conjugated to Alexa Fluor 488 secondary antibody, the sections were treated with 1% Sudan Black to reduce autofluorescence as a final step. The sections were analyzed by confocal microscopy (Zeiss 710 confocal microscope). For measurement of the number of PLA puncta, we counted the number of PLA puncta from 10 randomly selected areas within the dentate gyrus, CA3, CA1 or subiculum of each case. For each experiment, samples from an NCI, a mild and a severe AD case were examined, and the PLA signals were counted in each of the four areas. To determine how PLA counts changed as disease progressed, for each area, the numbers in the mild and severe AD sections were normalized to the number in the NCI section. Then, to assemble data from all cases, the PLA number from the NCI case in each experiment was set as 1 for each region. This allowed us to calculate an average PLA count for each region, using six cases of each disease state, and to determine how the level of association changed as disease progressed. To determine how PLA counts changed from region to region within a case, PLA counts from CA3, CA1, and subiculum were normalized to that of the DG, which was then given the value of '1'.

Flow cytometry

D5 cells were fixed and stained for flow cytometry following a protocol for detecting intracellular antigens (Krutzik and Nolan, 2003). Briefly, cells were treated with NGF (50 ng/ml) for 5 min and, after NGF treatment, adherent cells were fixed by adding 16% paraformaldehyde directly to the culture medium (1.5% paraformaldehyde final concentration) and incubating for 10 min. Fixed cells were trypsinized and pelleted, then permeabilized by vigorous resuspension in 3 ml ice-cold methanol for at least 10 min. Cells were washed with staining buffer (PBS with 1% BSA and 0.1% Tween 20) then incubated with primary antibody for 1 h. CP17 or non-specific mouse IgG antibodies (70 µg/ml, diluted in staining buffer) were used. After washing, cells were incubated with R-phycoerythrin (R-PE)-conjugated goat anti-mouse IgG [$F(ab')_2$ fragment, 1:200, A10543, Thermo Fisher Scientific] for 20 min. After washing, the cells were resuspended in staining buffer to a concentration of ~10^6 cells/ml and samples were analyzed with a Becton Dickinson LSRII cytometer. For data analysis, a gated population of 10,000 fluorescing cells was collected from each condition. The Cell Quest Pro software package was used to generate a histogram plot representing the fluorescence intensity of each cell in the population. The geometric mean fluorescence was calculated from each histogram. The fold-change in fluorescence intensity was calculated by dividing the geometric mean fluorescence of CP17-labeled samples from NGF-stimulated cells by that of CP17-labeled samples from non-stimulated cells. Background fluorescence from control IgG-labeled samples taken from NGF-stimulated or non-stimulated cells had been first subtracted.

Statistical analysis

To compare the SHP2-binding affinity between T231D and WT tau in the *in vitro* binding assays (Fig. 1D), statistical analysis was performed using a two-sample Student's *t*-test with the Statistical Analysis System software (SASS) package. The exact *P*-value is indicated. The increase in the level of endogenous tau-SHP2 complexes in NGF-stimulated PC6-3 cells was also statistically determined though a Student's *t*-test (Fig. 3E). To compare the level of CP17-labeled tau in PC6-3 cells before and after NGF treatment, the same statistical tests were carried out on data from three independent flow cytometry experiments. The exact *P*-value is indicated. To compare the fold increases of the number of tau-SHP2, T231D tau-SHP2, and T231A tau-SHP2 complexes detected by PLAs, statistical analysis was performed using analysis of variance (one-way ANOVA, linear mixed model) with the SASS package. In Fig. 5E, the data for each fold increase is shown as the mean± s.e.m. from three independent assays. The exact *P*-values are given.

The statistical analysis for fold increases in the number of tau-SHP2 complexes detected by PLA in human brain sections was also determined with a one-way ANOVA, followed by the honest significant difference (HSD) post hoc test. In Fig. 8B and Fig. S2, the data for each fold increase in the different hippocampal regions and subiculum were shown as the mean± s.e.m. The exact *P*-values are given.

Acknowledgements
We thank Dr Peter Davies for generously providing tau monoclonals DA9 and CP17. We also thank the University of Iowa Histology Research Lab for assistance. Some data in this paper formed part of a PhD thesis for Yohan Kim; the degree was conferred in May, 2017 by the Interdisciplinary Graduate Program in Molecular and Cellular Biology, The University of Iowa.

Competing interests
The authors declare no competing or financial interests.

Author contributions
Conceptualization: Y.K., G. Lee; Methodology: Y.K., G. Liu, G. Lee; Validation: Y.K., G. Liu, C.J.L., J.D.M., M.B.F.; Formal analysis: Y.K., C.J.L., J.D.M., M.B.F., M.M.H.; Investigation: Y.K., G. Liu, C.J.L., J.D.M., M.B.F.; Resources: M.M.H., J.A.S., G. Lee; Writing - original draft: Y.K., G. Lee; Writing - review & editing: G. Lee; Visualization: Y.K., G. Lee; Supervision: G. Lee; Project administration: G. Lee; Funding acquisition: G. Lee, G. Liu.

Funding
This work was supported by the National Institutes of Health [R01 AG017753 to G. Lee and F30 AG054134 to G. Liu], the Alzheimer's Association [IIRG-12-241042 to G. Lee], and a University of Iowa Neuroscience Institute Kwak–Ferguson Fellowship [to G. Liu]. Deposited in PMC for release after 12 months.

Supplementary information
Supplementary information available online at
http://jcs.biologists.org/lookup/doi/10.1242/jcs.229054.supplemental

References

Beaudoin, G. M., III, Lee, S.-H., Singh, D., Yuan, Y., Ng, Y.-G., Reichardt, L. F. and Arikkath, J. (2012). Culturing pyramidal neurons from the early postnatal mouse hippocampus and cortex. *Nat. Protoc.* **7**, 1741-1754. doi:10.1038/nprot.2012.099

Bhaskar, K., Yen, S.-H. and Lee, G. (2005). Disease-related modifications in tau affect the interaction between Fyn and Tau. *J. Biol. Chem.* **280**, 35119-35125. doi:10.1074/jbc.M505895200

Biernat, J., Gustke, N., Drewes, G., Mandelkow, E. M., and Mandelkow, E. (1993). Phosphorylation of Ser262 strongly reduces binding of tau to microtubules: distinction between PHF-like immunoreactivity and microtubule binding. *Neuron* **11**, 153-163. doi:10.1016/0896-6273(93)90279-z

Bramblett, G. T., Goedert, M., Jakes, R., Merrick, S. E., Trojanowski, J. Q. and Lee, V. M.-Y. (1993). Abnormal tau phosphorylation at Ser^{396} in Alzheimer's disease recapitulates development and contributes to reduced microtubule binding. *Neuron* **10**, 1089-1099. doi:10.1016/0896-6273(93)90057-X

Brandt, R. and Lee, G. (1993). Functional organization of microtubule-associated protein tau. Identification of regions which affect microtubule growth, nucleation, and bundle formation *in vitro*. *J. Biol. Chem.* **268**, 3414-3419.

Bryant, M. R., Marta, C. B., Kim, F. S. and Bansal, R. (2009). Phosphorylation and lipid raft association of fibroblast growth factor receptor-2 in oligodendrocytes. *Glia* **57**, 935-946. doi:10.1002/glia.20818

Dawson, H. N., Ferreira, A., Eyster, M. V., Ghoshal, N., Binder, L. I. and Vitek, M. P. (2001). Inhibition of neuronal maturation in primary hippocampal neurons from tau deficient mice. *J. Cell Sci.* **114**, 1179-1187.

De Borst, M. H., Prakash, J., Melenhorst, W. B. W. H., van den Heuvel, M. C., Kok, R. J., Navis, G. and van Goor, H. (2007). Glomerular and tubular induction of the transcription factor c-Jun in human renal disease. *J. Pathol.* **213**, 219-228. doi:10.1002/path.2228

Drewes, G., Trinczek, B., Illenberger, S., Biernat, J., Schmitt-Ulms, G., Meyer, H. E., Mandelkow, E. M., and Mandelkow, E. (1995). Microtubule-associated protein/microtubule affinity-regulating kinase (p110mark). A novel protein kinase that regulates tau-microtubule interactions and dynamic instability by phosphorylation at the Alzheimer-specific site serine 262. *J. Biol. Chem.* **270**, 7679-7688. doi:10.1074/jbc.270.13.7679

Esmaeli-Azad, B., McCarty, J. H. and Feinstein, S. C. (1994). Sense and antisense transfection analysis of tau function: tau influences net microtubule assembly, neurite outgrowth and neuritic stability. *J. Cell Sci.* **107**, 869-879.

Goedert, M., Jakes, R., Crowther, R. A., Six, J., Lubke, U., Vandermeeren, M., Cras, P., Trojanowski, J. Q. and Lee, V. M.-Y. (1993). The abnormal phosphorylation of tau protein at Ser-202 in Alzheimer disease recapitulates phosphorylation during development. *Proc. Natl. Acad. Sci. USA* **90**, 5066-5070. doi:10.1073/pnas.90.11.5066

Gu, H., Pratt, J. C., Burakoff, S. J. and Neel, B. G. (1998). Cloning of p97/Gab2, the major SHP2-binding protein in hematopoietic cells, reveals a novel pathway for cytokine-induced gene activation. *Mol. Cell* **2**, 729-740. doi:10.1016/S1097-2765(00)80288-9

Gustafsdottir, S. M., Schallmeiner, E., Fredriksson, S., Gullberg, M., Söderberg, O., Jarvius, M., Jarvius, J., Howell, M. and Landegren, U. (2005). Proximity ligation assays for sensitive and specific protein analyses. *Anal. Biochem.* **345**, 2-9. doi:10.1016/j.ab.2005.01.018

Hall, G. F., Yao, J. and Lee, G. (1997). Human tau becomes phosphorylated and forms filamentous deposits when overexpressed in lamprey central neurons in situ. *Proc. Natl. Acad. Sci. USA* **94**, 4733-4738. doi:10.1073/pnas.94.9.4733

Hernandez, P., Lee, G., Sjoberg, M. and Maccioni, R. B. (2009). Tau phosphorylation by cdk5 and Fyn in response to amyloid peptide Abeta (25-35): involvement of lipid rafts. *J. Alzheimers Dis.* **16**, 149-156. doi:10.3233/JAD-2009-0933

Herrup, K. and Yang, Y. (2001). Pictures in molecular medicine: contemplating Alzheimer's disease as cancer: a loss of cell-cycle control. *Trends Mol. Med.* **7**, 527. doi:10.1016/S1471-4914(01)02158-X

Hu, Y., Zheng, L., Cheng, L., Zhang, Y., Bai, W., Zhou, W., Wang, T., Han, Z., Zong, J., Jin, S. et al. (2017). GAB2 rs2373115 variant contributes to Alzheimer's disease risk specifically in European population. *J. Neurol. Sci.* **375**, 18-22. doi:10.1016/j.jns.2017.01.030

Inomata, M., Takayama, Y., Kiyama, H., Nada, S., Okada, M. and Nakagawa, H. (1994). Regulation of Src family kinases in the developing rat brain: correlation with their regulator kinase, Csk1. *J. Biochem.* **116**, 386-392. doi:10.1093/oxfordjournals.jbchem.a124536

Jicha, G. A., Lane, E., Vincent, I., Otvos, L., Jr, Hoffmann, R. and Davies, P. (1997). A conformation- and phosphorylation-dependent antibody recognizing the paired helical filaments of Alzheimer's disease. *J. Neurochem.* **69**, 2087-2095. doi:10.1046/j.1471-4159.1997.69052087.x

Kawarabayashi, T., Shoji, M., Younkin, L. H., Lin, W. L., Dickson, D. W., Murakami, T., Matsubara, E., Abe, K., Ashe, K. H. and Younkin, S. G. (2004). Dimeric amyloid beta protein rapidly accumulates in lipid rafts followed by apolipoprotein E and phosphorylated tau accumulation in the Tg2576 mouse model of Alzheimer's disease. *J. Neurosci.* **24**, 3801-3809. doi:10.1523/JNEUROSCI.5543-03.2004

Klein, C., Krämer, E.-M., Cardine, A.-M., Schraven, B., Brandt, R. and Trotter, J. (2002). Process outgrowth of oligodendrocytes is promoted by interaction of fyn kinase with the cytoskeletal protein tau. *J. Neurosci.* **22**, 698-707. doi:10.1523/JNEUROSCI.22-03-00698.2002

Krutzik, P. O. and Nolan, G. P. (2003). Intracellular phospho-protein staining techniques for flow cytometry: monitoring single cell signaling events. *Cytometry A* **55A**, 61-70. doi:10.1002/cyto.a.10072

Kusakari, S., Saitow, F., Ago, Y., Shibasaki, K., Sato-Hashimoto, M., Matsuzaki, Y., Kotani, T., Murata, Y., Hirai, H., Matsuda, T. et al. (2015). Shp2 in forebrain neurons regulates synaptic plasticity, locomotion, and memory formation in mice. *Mol. Cell. Biol.* **35**, 1557-1572. doi:10.1128/MCB.01339-14

Lacalle, R. A., Mira, E., Gómez-Moutón, C., Jiménez-Baranda, S., Martínez, A.-C. and Mañes, S. (2002). Specific SHP-2 partitioning in raft domains triggers integrin-mediated signaling via Rho activation. *J. Cell Biol.* **157**, 277-289. doi:10.1083/jcb.200109031

Lee, G. (2005). Tau and src family tyrosine kinases. *Biochim. Biophys. Acta* **1739**, 323-330. doi:10.1016/j.bbadis.2004.09.002

Lee, G. and Rook, S. L. (1992). Expression of tau protein in non-neuronal cells: microtubule binding and stabilization. *J. Cell Sci.* **102**, 227-237.

Lee, G., Newman, S. T., Gard, D. L., Band, H. and Panchamoorthy, G. (1998). Tau interacts with src-family non-receptor tyrosine kinases. *J. Cell Sci.* **111**, 3167-3177.

Lee, G., Thangavel, R., Sharma, V. M., Litersky, J. M., Bhaskar, K., Fang, S. M., Do, L. H., Andreadis, A., Van Hoesen, G. and Ksiezak-Reding, H. (2004). Phosphorylation of tau by fyn: implications for Alzheimer's disease. *J. Neurosci.* **24**, 2304-2312. doi:10.1523/JNEUROSCI.4162-03.2004

Leugers, C. J. and Lee, G. (2010). Tau potentiates nerve growth factor-induced mitogen-activated protein kinase signaling and neurite initiation without a requirement for microtubule binding. *J. Biol. Chem.* **285**, 19125-19134. doi:10.1074/jbc.M110.105387

Lindwall, G. and Cole, R. D. (1984). Phosphorylation affects the ability of tau protein to promote microtubule assembly. *J. Biol. Chem.* **259**, 5301-5305.

Nagy, Z. (2000). Cell cycle regulatory failure in neurones: causes and consequences. *Neurobiol. Aging* **21**, 761-769. doi:10.1016/S0197-4580(00)00223-2

Pei, J.-J., Braak, H., An, W.-L., Winblad, B., Cowburn, R. F., Iqbal, K. and Grundke-Iqbal, I. (2002). Up-regulation of mitogen-activated protein kinases ERK1/2 and MEK1/2 is associated with the progression of neurofibrillary degeneration in Alzheimer's disease. *Brain Res. Mol. Brain Res.* **109**, 45-55. doi:10.1016/S0169-328X(02)00488-6

Pittman, R. N., Wang, S., DiBenedetto, A. J., and Mills, J. C. (1993). A system for characterizing cellular and molecular events in programmed neuronal cell death. *J. Neurosci.* **13**, 3669-3680. doi:10.1523/JNEUROSCI.13-09-03669.1993

Raina, A. K., Zhu, X. and Smith, M. A. (2004). Alzheimer's disease and the cell cycle. *Acta Neurobiol. Exp. (Wars.)* **64**, 107-112.

Reiman, E. M., Webster, J. A., Myers, A. J., Hardy, J., Dunckley, T., Zismann, V. L., Joshipura, K. D., Pearson, J. V., Hu-Lince, D., Huentelman, M. J. et al. (2007). GAB2 alleles modify Alzheimer's risk in APOE epsilon4 carriers. *Neuron* **54**, 713-720. doi:10.1016/j.neuron.2007.05.022

Sarkar, M., Kuret, J. and Lee, G. (2008). Two motifs within the tau microtubule-binding domain mediate its association with the hsc70 molecular chaperone. *J. Neurosci. Res.* **86**, 2763-2773. doi:10.1002/jnr.21721

Seward, M. E., Swanson, E., Norambuena, A., Reimann, A., Cochran, J. N., Li, R., Roberson, E. D. and Bloom, G. S. (2013). Amyloid-beta signals through tau to drive ectopic neuronal cell cycle re-entry in Alzheimer's disease. *J. Cell Sci.* **126**, 1278-1286. doi:10.1242/jcs.1125880

Sharma, V. M., Litersky, J. M., Bhaskar, K. and Lee, G. (2007). Tau impacts on growth-factor-stimulated actin remodeling. *J. Cell Sci.* **120**, 748-757. doi:10.1242/jcs.03378

Shi, Z.-Q., Yu, D.-H., Park, M., Marshall, M. and Feng, G.-S. (2000). Molecular mechanism for the Shp-2 tyrosine phosphatase function in promoting growth factor stimulation of Erk activity. *Mol. Cell. Biol.* **20**, 1526-1536. doi:10.1128/MCB.20.5.1526-1536.2000

Söderberg, O., Gullberg, M., Jarvius, M., Ridderstråle, K., Leuchowius, K.-J., Jarvius, J., Wester, K., Hydbring, P., Bahram, F., Larsson, L.-G. et al. (2006). Direct observation of individual endogenous protein complexes in situ by proximity ligation. *Nat. Methods* **3**, 995-1000. doi:10.1038/nmeth947

Söderberg, O., Leuchowius, K.-J., Gullberg, M., Jarvius, M., Weibrecht, I., Larsson, L.-G. and Landegren, U. (2008). Characterizing proteins and their interactions in cells and tissues using the in situ proximity ligation assay. *Methods* **45**, 227-232. doi:10.1016/j.ymeth.2008.06.014

Sugimoto, S., Wandless, T. J., Shoelson, S. E., Neel, B. G. and Walsh, C. T. (1994). Activation of the SH2-containing protein tyrosine phosphatase, SH-PTP2, by phosphotyrosine-containing peptides derived from insulin receptor substrate-1. *J. Biol. Chem.* **269**, 13614-13622.

Tajan, M., de Rocca Serra, A., Valet, P., Edouard, T. and Yart, A. (2015). SHP2 sails from physiology to pathology. *Eur. J. Med. Genet.* **58**, 509-525. doi:10.1016/j.ejmg.2015.08.005

Tremblay, M. A., Acker, C. M. and Davies, P. (2010). Tau phosphorylated at tyrosine 394 is found in Alzheimer's disease tangles and can be a product of the Abl-related kinase, Arg. *J. Alzheimers Dis.* **19**, 721-733. doi:10.3233/JAD-2010-1271

Vincent, I., Zheng, J.-H., Dickson, D. W., Kress, Y. and Davies, P. (1998). Mitotic phosphoepitopes precede paired helical filaments in Alzheimer's disease. *Neurobiol. Aging* **19**, 287-296. doi:10.1016/S0197-4580(98)00071-2

Wang, W., Bu, B., Xie, M., Zhang, M., Yu, Z. and Tao, D. (2009). Neural cell cycle dysregulation and central nervous system diseases. *Prog. Neurobiol.* **89**, 1-17. doi:10.1016/j.pneurobio.2009.01.007

Weaver, C. L., Espinoza, M., Kress, Y. and Davies, P. (2000). Conformational change as one of the earliest alterations of tau in Alzheimer's disease. *Neurobiol. Aging* **21**, 719-727. doi:10.1016/S0197-4580(00)00157-3

Webber, K. M., Raina, A. K., Marlatt, M. W., Zhu, X., Prat, M. I., Morelli, L., Casadesus, G., Perry, G. and Smith, M. A. (2005). The cell cycle in Alzheimer disease: a unique target for neuropharmacology. *Mech. Ageing Dev.* **126**, 1019-1025. doi:10.1016/j.mad.2005.03.024

Weingarten, M. D., Lockwood, A. H., Hwo, S. Y. and Kirschner, M. W. (1975). A protein factor essential for microtubule assembly. *Proc. Natl. Acad. Sci. USA* **72**, 1858-1862. doi:10.1073/pnas.72.5.1858

Witman, G. B., Cleveland, D. W., Weingarten, M. D. and Kirschner, M. W. (1976). Tubulin requires tau for growth onto microtubule initiating sites. *Proc. Natl. Acad. Sci. USA* **73**, 4070-4074. doi:10.1073/pnas.73.11.4070

Wright, J. H., Drueckes, P., Bartoe, J., Zhao, Z., Shen, S. H. and Krebs, E. G. (1997). A role for the SHP-2 tyrosine phosphatase in nerve growth-induced PC12 cell differentiation. *Mol. Biol. Cell* **8**, 1575-1585. doi:10.1091/mbc.8.8.1575

Zhang, J., Zhang, F. and Niu, R. (2015). Functions of Shp2 in cancer. *J. Cell. Mol. Med.* **19**, 2075-2083. doi:10.1111/jcmm.12618

Zhu, X., Lee, H.-G., Raina, A. K., Perry, G. and Smith, M. A. (2002). The role of mitogen-activated protein kinase pathways in Alzheimer's disease. *NeuroSignals* **11**, 270-281. doi:10.1159/000067426